Available online at www.sciencedirect.com

ScienceDirect

Procedia Materials Science 11 (2015) 381 – 385

Procedia Materials Science

www.elsevier.com/locate/procedia

5th International Biennial Conference on Ultrafine Grained and Nanostructured Materials, UFGNSM15

Synthesizing of Nanostructured Fe-Mn Alloys by Mechanical Alloying Process

N. Safaie[a], M. Khakbiz[a,*], S. Sheibani[b], P. Sotoudeh Bagha[a]

[a] *Division of Biomedical Engineering, Department of Life Science Engineering, Faculty of New Sciences and Technologies, University of Tehran, North Karegar Ave., P.O. Box 14395-1561, Tehran, Iran*

[b] *School of Metallurgy and Materials Engineering, College of Engineering, University of Tehran, North Karegar Ave., P.O. Box 11155-4563, Tehran, Iran*

Abstract

In the present study, nanostructured Fe-30 wt.% Mn alloys produced by mechanical alloying of Fe and Mn powders mixture. The phase composition and morphology of nanostructured powder were analyzed by X-ray diffraction and scanning electron microscopy. It was found that by milling time up to 10h, crystallite size was decreased to 6 nm, on the contrary lattice strain was increased. Solid solubility levels were determined from changes in the lattice parameter values. The lattice parameter increases slightly from 0.28167 to 0.35776 nm. Increasing milling intensity by higher ball to powder mass ratio resulted in Fe-Mn alloy formation with smaller crystallite size. The SEM results showed that, plate like particles were formed in initial milling time and particles morphology was changed to equiaxed form in final stage of milling process.

Peer-review under responsibility of the organizing committee of UFGNSM15

Keywords: Mechanical Alloying; Nanostructured Fe-Mn Alloy; X-ray diffraction.

1. Introduction

Ball milling technique has been used to take solid state reaction at near room temperature. In mechanical alloying technique amorphous phases and super saturated solid solution are available, Suryanarayana (2001). Fe-Mn alloy is one of the interesting alloys in biodegradable biomaterials which are expected to support healing process of a

* Corresponding author. Tel.: +982161118472; fax: +982188617087.
E-mail address: khakbiz@ut.ac.ir

Peer-review under responsibility of the organizing committee of UFGNSM15
doi:10.1016/j.mspro.2015.11.134

diseased tissue and to degrade thereafter, Hermawan et al. (2010). There are some papers in which data related to Fe-Mn alloys obtained by mechanical alloying, Cherdyntsev and Kaloshkin (2010), Cotes et al. (2002), Tcherdyntsev et al. (2006). Single phase FCC structure for Fe-30%Mn and Fe-35%Mn composition were proposed by Hermawan et al. (2008), because of non-ferromagnetic properties which results in compatibility with magnetic resonance imaging that is desired for medical application. Iron base alloys have been used for clinical stent implantation, Peuster et al. (2006) because of their good mechanical properties, biocompatibility, also biodegradable properties, which can be absorbed in body without foreign body reactions, Hermawan and Mantovani (2013), Schinhammer et al. (2013), Hermawan et al. (2010), Drynda et al. (2015).

Due to the special properties of nanostructured alloys it is essential to synthesis Fe-Mn alloy by mechanical alloying that was not studied by other researchers for biomedical applications. In present study, X-ray diffraction (XRD), Scanning Electron Microscopy (SEM) and Energy Dispersive Spectrometry (EDS) has evidenced the formation of nanostructured Fe-30Mn alloy that can be used as biodegradable powder in production of medical implants. Milling time and ball to powder mass ratio are important factors for achieving the desired particle size and single FCC phase of milled powders.

2. Experimental

The Fe-Mn alloys with Fe-30%wt Mn were prepared by ball milling of Fe and Mn elemental powders of about 99.9% purity in a planetary high energy ball milling (PM2400) using hardened steel balls and vial. Milling process was performed under argon atmosphere with the rotation speed of 250 rpm by addition of 10 ml of toluene as processing control agent. Milling of powder with two different ball-to-powder mass ratios of 20 (called hereafter S20 sample) and 30 (called hereafter S30 sample) was examined. The amount of balls and mass of raw mixture were adjusted proportionally during changes of ball-to-powder mass ratios. The size of balls (diameter) were 10 and 15mm for all milling runs. XRD analysis was performed by using a Philips PW-3710 diffractometer with Cu k_{α} radiation. The crystallite size and lattice strain of milled powder was calculated by Williamson-Hall equation, Williamson and Hall (1953). Lattice parameter can be obtained from shifts in peak positions in the XRD patterns, Sivasankaran et al. (2011). The morphology of the products was examined by a SEM VEGA3-XMU TESCAN equipped with EasyEDX EDS.

3. Results and discussion

3.1. XRD analysis

Figure 1 shows the XRD patterns after different milling times. Initial powder mixture shows α-Fe (BCC) and α-Mn (BCC). It can be found that, S20 sample after different milling times of 5 and 10h show α-Fe. To ensure solid solubility and enriching the γ-Fe (FCC) nonmagnetic phase, ball to powder mass ratio increased to 30 in S30 sample. It can be seen in Fig. 1 that, 5h milling of S30 sample results in both α-Fe and γ-Fe phases. However, by increasing of milling time to 10h only nonmagnetic γ-Fe phase appears and α-Mn disappears completely.

Crystallite size, lattice strain and lattice parameter of different samples calculated from XRD data are summarized in Table 1. It can be seen that for both S20 and S30 samples, by increasing milling time from 5 to 10h, the crystallite size decreased and lattice strain increased. Furthermore, higher milling energy with ball to powder mass ratio of 30 compared to 20, shows smaller crystallite size and higher lattice strain. Therefore, higher milling energy shortens the diffusion paths required for Fe-Mn solid solution formation.

3.2. Morphology analysis

The typical SEM images of initial powder mixture and 10h milled S30 sample are presented in Fig. 2. Fig. 2a shows the SEM image of initial Fe-Mn powders mixture. Relatively large plate-like particles and small particles exhibit wide size distribution in this powders mixture. As the milling time increased to 10h (see Fig. 2b), the particles shape underwent changes from plate-like structure to equaxied. Also the average particles size was reduced

by milling. The formation of relatively large and loose agglomerates may be attributed to the crystal structure of Fe and Mn in which particles are easily deformed and cold welded to each other.

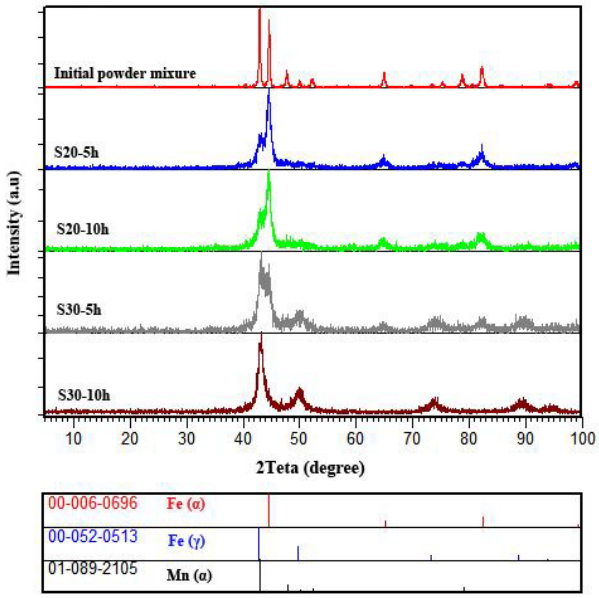

Fig. 1. XRD patterns of initial powder mixture, S20 and S30 samples after different milling times of 5 and 10h.

Table 1. Crystallite size, lattice strain and lattice parameter of different samples.

sample	Crystallite Size (nm)	Lattice Strain (%)	Latticte Parameter (nm)
Initial powder mixture	-	-	2.8167
S20-5h	60	0.19	2.817
S20-10h	16	0.61	2.8298
S30-5h	14	1.49	2.595
S30-10h	6	1.93	3.5776

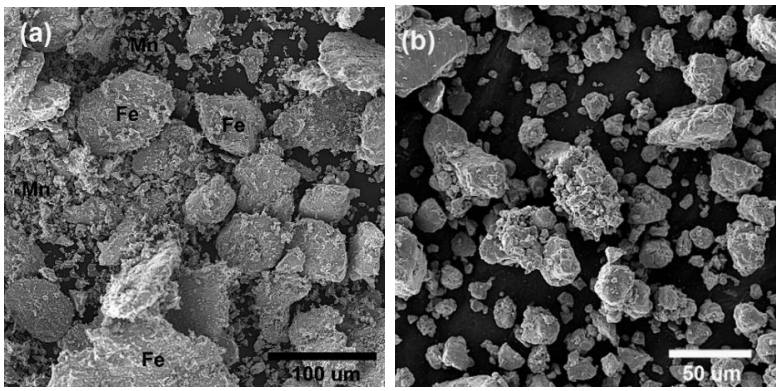

Fig. 2. SEM images of (a) initial powder mixture; and (b) 10h milled S30 sample.

Figure 3 shows the 10 h milled S30 microstructure and corresponding X-ray mapping images of Fe and Mn elements. In the mapping analysis, it can be seen that all the elements were homogeneously distributed on an atomic scale. As shown in the XRD pattern of the final product (Fig. 1), these elements are in the form of Fe-Mn solid solution.

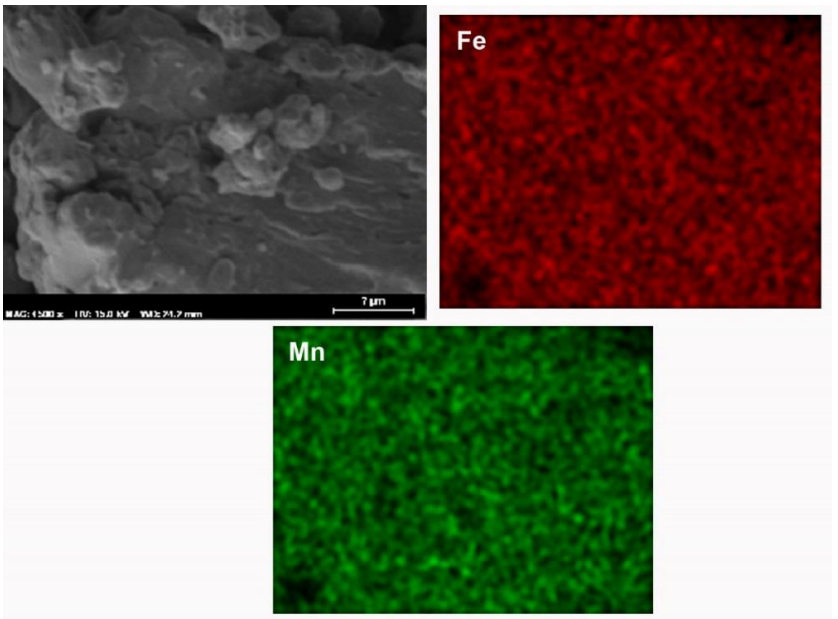

Fig. 3. SEM image of 10 h milled S30 sample and the corresponding Fe and Mn mapping.

4. Conclusion

In this research, the effect of different parameters of ball to powder mass ratio and milling time on Fe-Mn solid solution formation using high energy ball milling was studied. The nanostructured Fe-30 wt.% Mn alloy synthesized after 10h milling and evaluated by XRD and SEM techniques. Crystallite size, lattice strain and lattice parameter of different samples estimated from XRD data. The increase of milling energy by increasing ball to powder mass ratio and milling time caused better solid solubility. Results indicated that 10h of milling and ball to powder mass ratio of 30 can produce powders by crystallite size of 6 nm. It can be found that all the elements were homogeneously distributed on an atomic scale.

References

Cherdyntsev, V. V., Kaloshkin, S.D., 2010. On the Kinetics of Phase and Structural Transformations upon Mechanical Alloying. The Physics of Metals and Metallography 109, 492–504.

Cotes, S.M., Cabrera, A.F., Damonte, L.C., Mercader, R.C., Desimoni, J., 2002. Magnetic Properties of Ball-Milled Fe–Mn Alloys. Physica B: Condensed Matter 320, 274–277.

Drynda, A., Hassel, T., Bach, F.W., Peuster, M., 2015. In Vitro and in Vivo Corrosion Properties of New Iron-Manganese Alloys Designed for Cardiovascular Applications. Journal of Biomedical Materials Research. Part B, Applied Biomaterials 103, 649–60.

Hermawan, H., Alamdari, H., Mantovani, D., Dubé, D., 2008. Iron–Manganese: New Class of Metallic Degradable Biomaterials Prepared by Powder Metallurgy. Powder Metallurgy 51, 38–45.

Hermawan, H., Dubé, D., Mantovani, D., 2010. Degradable Metallic Biomaterials: Design and Development of Fe-Mn Alloys for Stents. Journal of Biomedical Materials Research Part A 93A, 1–11.

Hermawan, H., Mantovani, D., 2013. Process of Prototyping Coronary Stents from Biodegradable Fe-Mn alloys. Acta Biomaterialia 9, 8585–92.

Peuster, M., Hesse, C., Schloo, T., Fink, C., Beerbaum, P., von Schnakenburg, C., 2006. Long-Term Biocompatibility of a Corrodible Peripheral Iron Stent in the Porcine Descending Aorta. Biomaterials 27, 4955–62.

Schinhammer, M., Gerber, I., Hänzi, A.C., Uggowitzer, P.J., 2013. On the Cytocompatibility of Biodegradable Fe-Based Alloys. Materials Science & Engineering. C, Materials for Biological Applications 33, 782–9.

Sivasankaran, S., Sivaprasad, K., Narayanasamy, R., Satyanarayana, P.V., 2011. X-ray Peak Broadening Analysis of AA 6061100−x−xwt.% Al2O3 Nanocomposite Prepared by Mechanical Alloying. Materials Characterization 62, 661–672.

Suryanarayana, C., 2001. Mechanical Alloying and Milling. Progress in Materials Science 46, 1–184.

Tcherdyntsev, V. V., Pustov, L.Y., Kaloshkin, S.D., Shelekhov, E. V., Principi, G., 2006. Phase Coexistence in Mechanicallly Alloyed Iron–Manganese Powders. Hyperfine Interactions 168, 937–942.

Williamson, G. K., Hall, W. H., 1953.